CFD based analysis of drag forces on twin submerged floating tubes

F. Forghanjaya[1], J. Akmal[2,*], A. Lubis[2], H. Harmen[2], M. Irsyad[2], M. B. Ramadhan[2]

[1] Mechanical Engineering Department, Universitas Lampung, Tunas Garuda Polytechnic, Indonesia
[2] Mechanical Engineering Department, Universitas Lampung, Indonesia

ABSTRACT: Twin submerged floating tubes (Twin-SFT) are widely found in structural applications, e.g. underwater cables, piping systems, even recently a lot of research has been directed towards transport tunnels. Currently, research on Twin-SFT is still limited and far behind when compared to single tubes. This research aims to observe the drag force on Twin-SFT. The study investigates the effect of the axis distance between the tubes, the diameter, and the depth of the installation of the double-tube structure on the drag force. The diameter variations of the tubes are 2 in (50.8 mm), 2 ½ in (63.5 mm) and 3 in (76.2 mm), each with a length of 600 mm. The tubes were mounted parallel to the centre distance between the upstream and downstream cylinders at x/L = 1⁄4, x/L = 1⁄2, x/L = 3⁄4 and x/L = 1, where x/L is the ratio of distance to wavelength (L). To assess the influence of the installation depth, the tubes were mounted at depths of 100 mm and 200 mm. The results showed that the drag forces on both cylinders were smallest at a distance of x/L = 1⁄4. Additionally, as the tube's depth increases, the drag force decreases, while larger tube diameters result in greater drag force.

KEYWORDS: Twin-SFT, CFD based analysis, Wavelength, Drag force, Streamline.

[Received April 14, 2024; Revised July 15, 2024; Accepted Sept. 9, 2024] Print ISSN: 0189-9546 | Online ISSN: 2437-2110

I. INTRODUCTION

Submerged Floating Tunnel (SFT) is a new concept that can be a solution for crossing transportation routes in straits or lakes, where it is not possible to make conventional bridges (Arthi and Murugeshwari, 2012; Mascella, 2020). Compared to conventional bridges and tunnels, SFT has many advantages (Jiang et al, 2018), including low construction costs, fast construction time, environmentally friendly, portable and reusable materials (Budiman, 2017). In addition to being useful in transportation (Zambon, 2019), similar concepts can be used for cable lines and underwater pipelines (Shankar et al, 1988); Cheng et al, 2012). It is expected that the structure shows stable behaviour under the action of currents and waves, thus reducing the need for additional design solutions to eliminate uncontrolled movement (Popov et al, 2018).

Like other offshore structures, ocean waves are a major disturbance to the SFT structures. This disruption will be significant for SFTs located in areas with strong currents and high waves. This disturbance can cause excessive vibration on the structure. There is an excitation force caused by the instability of the current characterized by the occurrence of a periodic water vortex, which will cause the emergence of vibrations on the structure of the cylinder. Furthermore, such vibrations can increase the force of the barrier that works on the structure. If this continues to happen, fatigue damage can occur to the structure (Bearman, 2011).

Research on Twin-SFT is currently limited and not as advanced compared to single tubes. There is a noticeable gap in both data and understanding between these two areas. As a consequence, the study of twin-tubes has not progressed as swiftly or extensively. While existing research on single tubes offers valuable insights, the distinct characteristics of twin-tubes necessitate focused investigation. Drag force is a crucial factor that affects the stability and performance of these structures (Deng, 2020). By studying this force, we can better understand the behaviour of twin-tubes in underwater environments. This understanding is vital for enhancing their design and functionality.

This research aims to determine the drag force received by the upstream and downstream tube, respectively. The key geometric variable under study is the ratio of the distance between cylinders (x) to the wavelength (L). Additionally, the research examines the influence of changes in tube diameter and depth from the water surface. The discussion is related to various aspects including streamline flow, drag coefficient and Reynolds number. The outcomes of this research will contribute to the broader field of marine engineering, addressing the knowledge gap between single and twin-tube structures. Ultimately, this study seeks to provide essential data that will support further advancements in Twin-SFT technology.

II. THEORETICAL FRAMEWORK

In fluid dynamics, the in-line force of a wave can be calculated using the Morison equation (Morison *et al*, 1950). The Morison equation is a semi-empirical equation commonly

*Corresponding author: jamiatul.akmal@eng.unila.ac.id
doi: http://dx.doi.org/10.4314/njtd.v21i4.2554

used to estimate the wave load on the design of oil platforms and offshore structures (Triatmodjo, 1999). Two small-scale experiments were conducted to see the accuracy of the Morison equation with actual load, with the final result that this equation was highly effective for both vertical and horizontal cylinders (Boccotti *et al*, 2012). Hence, the Morison equation is also effectively applied to SFT structures that are immersed horizontally along the sea. This is a simulation to see the received drag force of a twin cylinder mounted parallel and vertical to the direction of the wave.

The speed of the water particle is calculated using Morison's theory as presented in Equation (1) (Morison *et al*, 1950), where the orbital velocity of the horizontal direction obtained by means of differential results against time is formulated as:

$$u = \frac{\pi H}{T} \cdot \frac{cosh\ \frac{2\pi}{L}(d+z)}{sinh\ \frac{2\pi d}{L}} \cdot cos\ \frac{2\pi t}{T} \quad (1)$$

Here, u is the velocity of the water particle in the direction of x, whereas the values of H, T, d, z, and L refer to Table 1. The drag force equation which is one of the components of the Morison force can be written as shown in Equation (2).

$$F_D = \frac{1}{2} C_D . \rho . \mathrm{D} . u^2 . l \quad (2)$$

CD is the drag coefficient and ρ is the fluid density. The CD values for this study are taken from a table that has been compiled and recommended by the United States Army Coast Technical Center, which refers to many of the results of laboratory experiments, as shown in Table 1 (Reeve et al, 2016).

Table 1. Values of C_D and C_M recommendations of the U.S. Army Coastal Engineering Center (Sumer and FredsØe, 2006)

Reynolds number	C_M
$R < 2.5 \times 10^5$	2.0
$2.5 \times 10^5 < R < 5 \times 10^5$	$C_M = 2.5 - R/(5 \times 10^5)$
$R > 5 \times 10^5$	$C_M = 1.5$

Reynolds number	C_D
$R < 10^5$	1.2
$10^5 < R < 4 \times 10^5$	$1.2 < C_D < 0.6$
$R > 4 \times 10^5$	$C_D = 0.6–0.7$

The size of the C_D drag coefficient in Table 2 is determined by the Reynolds number, expressed by Equation (3), where U and v represent the velocity value and the kinematic viscosity of the fluid.

$$Re = \frac{UD}{v} \quad (3)$$

The Reynolds number is a parameter for determining the type of flow around the cylinder, so the value will vary according to the flow type that occurs. Many experiments have been carried out to determine the influence of Reynolds number on the coefficient of pull, such as those done by (Schlichting, 1979; Sarpkaya, 2010). One of the research results is shown in Figure 1.

The value of velocity values (u) for depth variations can be seen in Table 2, and used as a velocity inlet parameter, i.e. on the part of the velocity magnitude. The outlet limit condition is set to the pressure outlet type, whereas the other limit conditions are set to wall type (ANSYS Inc., 2022). Both of these velocity values are subsequently used to obtain the Reynolds number.

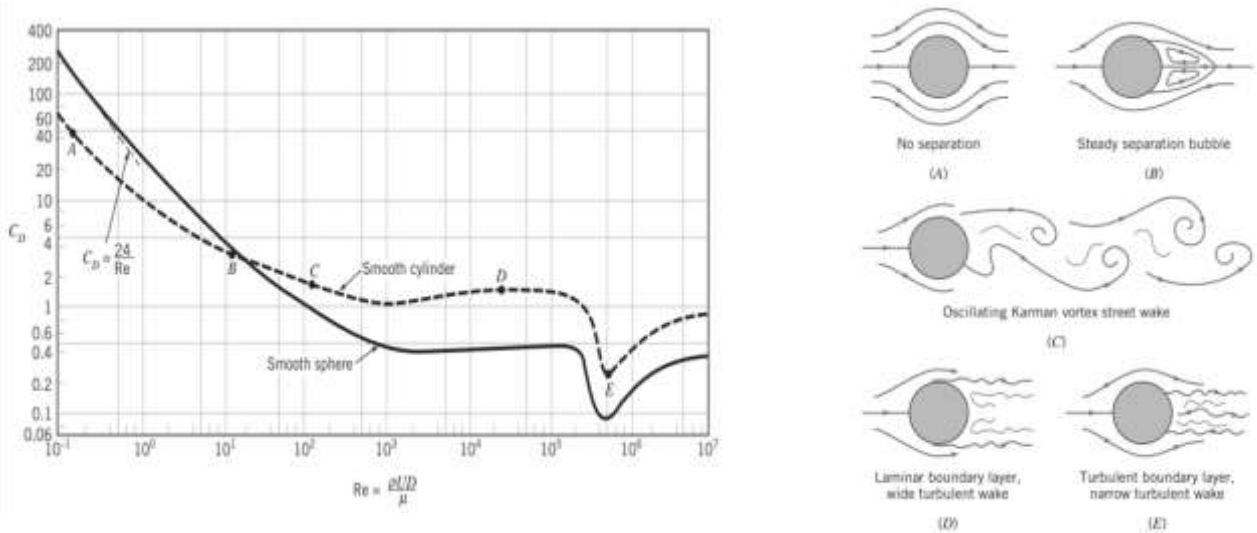

(a) (b)

Figure 1. (a) Graphic Value of drag coefficient (drag) for circular cylinders as a function of the Reynolds number (b) Type of flow pattern (Munson et al, 2022).

This study uses the fluid configuration Volume of Fluid (VOF) – Open Channel Wave Boundaries, because of the two types of fluid used: air and water (ANSYS Inc., 2021). The *k-ω SST* model has better accuracy when used to model the flow. The *k-ω SST* is also more reliable for the wider flow class than the *k-ω Standard* (Adanta *et al*, 2020; Mulvany *et al*, 2004). The solution method used in this simulation is Pressure-Velocity Coupling with the SIMPLE scheme (Semi Implicit Method for Pressure Linked Equations). The output for the report definition was set to drag force for upstream and downstream cylinders as research data for further analysis.

Table 2. Research Parameter Value of *Re*

z(mm)	D (mm)	u(mm/s)	Re
100	3 in (76.2)	82.7	6270.33
	2.5 in (63.5)	82.7	5225.27
	2 in (50.8)	82.7	4180.22
200	3 in (76.2)	28.4	2153.29
	2.5 in (63.5)	28.4	1794.41
	2 in (50.8)	28.4	1435.53

III. METHODOLOGY

This research used a numerical computational method with ANSYS Fluent 2023R1 (student version) in three stages: pre-processing, processing, and post-processing. The model is considered Volume of Fluid (VoF)-Open Channel Wave BC. The meshing sizes of the media and tube are 50 mm and 20 mm, respectively, as seen in Figure 2 (a). Boundary conditions consist of; a tube wall, media wall, inlet, and outlet, as seen in Figure 2 (b).

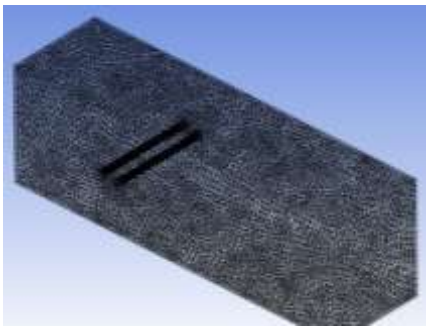

(a)

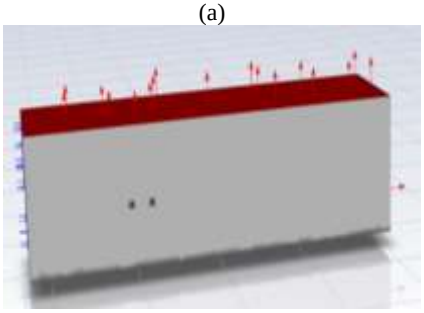

(b)

Figure 2. CFD Model: (a) Meshing element and (b) Boundary conditions.

The analysis parameters refer to Figure 2 where the value of T wave period and the total depth (d) are 0.625 seconds and 600 mm. The values of the other parameters used in this study are summarized in Table 1. The entire computing domain with boundary is shown in Figure 3, where d is the depth of the water, z is the distance of the center of the cylinder from the still water level, and six types of associated limit conditions: inlet, outlet, wall, sky (atmosphere), upstream and downstream cylinders (ANSYS Inc., 2015). The Inlet boundary condition is defined as Velocity Inlet (ANSYS Inc., 2022) which is related to wave height, base depth, and wavelength. The complete experimental parameter design is shown in Table 3, where these parameters are based on the wave pool produced in previous research (Akmal *et al*, 2022).

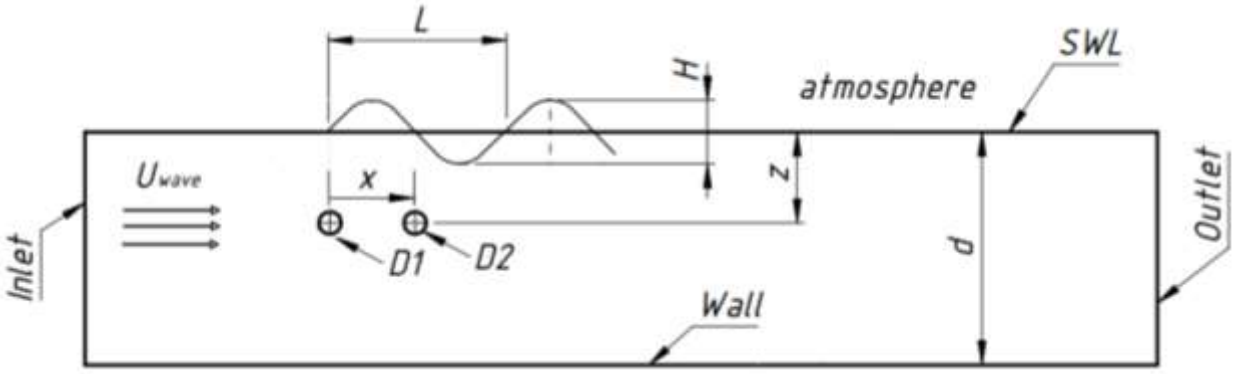

Figure 3. Computational domain scheme and boundary area.

Table 3. Parameters Data

No	Cylinder depth immersed *z, mm*	Cyl. Diameter *D,* Inch (mm)	Distance between Cyl. *x/L (mm)*
1	100	3 in (76.2)	¼ (146.75)
2			½ (293.5)
3			¾ (440.25)
4			1 (587)
5		2.5 in (63.5)	¼ (146.75)
6			½ (293.5)
7			¾ (440.25)
8			1 (587)
9		2 in (750.8)	¼ (146.75)
10			½ (293.5)
11			¾ (440.25)
12			1 (587)
13	200	3 in (76.2)	¼ (146.75)
14			½ (293.5)
15			¾ (440.25)
16			1 (587)
17		2.5 in (63.5)	¼ (146.75)
18			½ (293.5)
19			¾ (440.25)
20			1 (587)
21		2 in (750.8)	¼ (146.75)
22			½ (293.5)
23			¾ (440.25)
24			1 (587)
Tube length *l*, mm			600
Wavelength *L*, mm			587
Wave height *H*, mm			48
Period *T*, s			0,625

IV. RESULTS AND DISCUSSION

To determine the accuracy of the CFD simulation, a comparative study was conducted with the theoretical based on equation (2), as can be seen in Table 4. This study was carried out on a 3 in diameter tube placed at a level of depth of 100 mm.

Table 4. Drag Force Results Simulation and Calculation on Single Cylinder

CFD Analysis	Theoretical [10]	Difference
0.16757 N	0.18737 N	6.7151%

A. The effect of the distance between the two tubes (x/L) on the drag force

Figure 4 shows the drag force received on each tube. It turns out that the smaller the distance between the two tubes, the less the drag force is. At a distance x = L upstream and downstream cylinders each get the greatest drag force compared to the other distance variations. Shown that the trend that the drag force received by both cylinders' decreases, ranging from the cylinder gap x/L = 1 to x/L = ¼. The study revealed that the separation of the flow between two cylinders, influenced by the distance parameters, leads to a low-pressure turbulent area called a wake region. In this area, vortex formation and shedding occur, causing fluctuations in flow velocity and pressure distribution, thus forming a turbulence zone and changing the flow pattern, as shown in Figure 5. The greatest drag force difference between cylinders exists at the axis distance variation x/L = ¼. This is caused by the very close distance between the cylinders, the separated flow does not pass through the front of the downstream cylinder, but the previous flow merges or re-unites in the back of the downstream cylinder. As a result, the drag force that occurs in the downstream cylinder is very small, even negative or reverse-directional, where this is possible because there is no wave flow in the area between the two cylinders. Increasing the gap between the cylinders will make the aggregate position of the current in front of the downstream cylinder, so that the flow will hit the front surface of the downstream cylinder and result in an increased drag force on that cylinder.

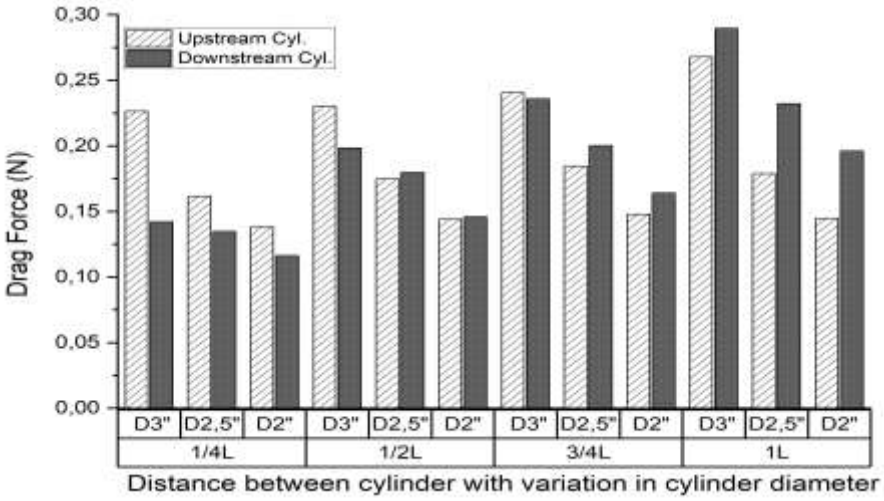

Figure 4. Graphic Value of Drag Force on Upstream and Downstream Cylinders with Variation of Cylinder Intervals for Diameter 3 in, 2.5 in and 2 in for depth level z = 100 mm

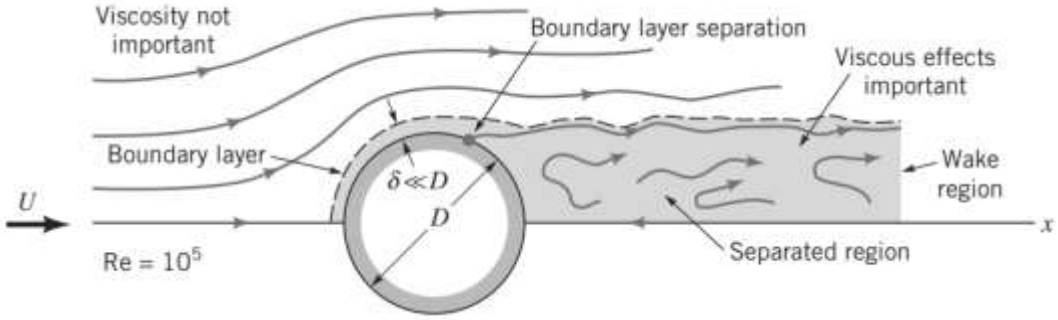

Figure 5. The flow character that passes through the cylinder (Munson, 2022)

.

In addition, there is the effect of position of each tube at phases differences of the wave, depending on the distance between the tubes. The different position of the phase of wave for each tube can be described in Figure 6. For example, at the distance x/L = 1⁄2 occurs a phase difference of 180 degrees where when the crest of a wave is above the upstream cylinder then the position of a trough of the wavelength is over the downstream. Thus, the resultant force that occurs at different phases should be the smallest in comparison with the other phases. In contrast, for x/L = 1 there is no different phase so that both cylinders are exposed to waves at the same phase and the resulting drag force which occurs will be the largest. However, there is an anomaly that at the distance x/L = 1⁄2 there is a resultant drag force that is greater than the distance x/L = 1⁄4, in which case it can be explained that the influence of the turbulence on the Wake area behind the upstream cylinder is larger than that of the difference phase. The total drag force on the upstream and downstream cylinders is an important data for SFT, which can be used in the global statistical analysis of the entire structure (Deng, 2020). Based on these findings, it can be recommended that in designing Twin SFT to consider the optimal distance between the two tubes. In this case the recommended distance ratio is x/L= 1/4 or 1/2.

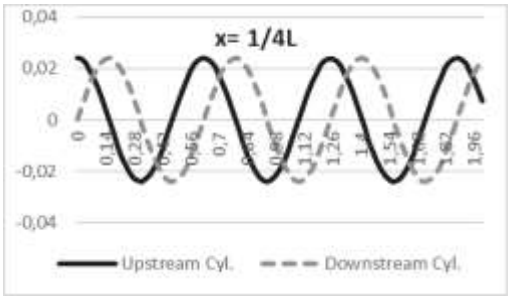

(a)

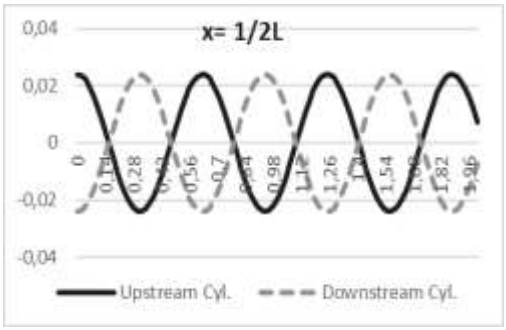

(b)

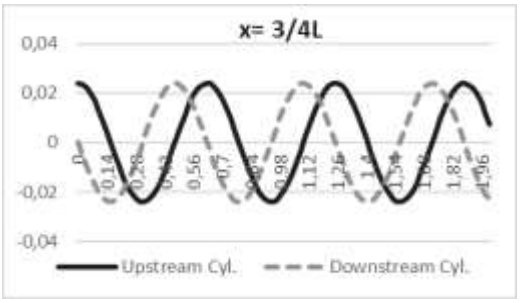

(c)

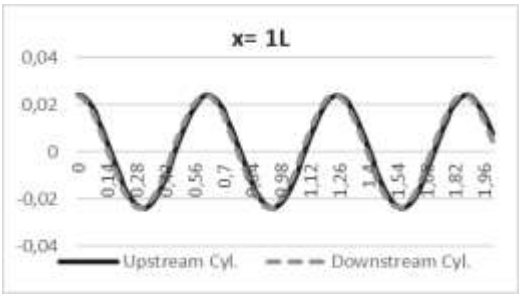

(d)

Figure 6. Phase differences of the cylinder with the variation of the distance between the axis of cylinders: a) x/L= 1⁄4, b) x/L = 1⁄2, c) x/L = 3⁄4, d) x/L = 1

The effect of the diameter on the drag force is the smaller the cylinder diameter, the smaller is the drag value. This is due to a drag force that is direct relative to the projection area of the object as shown by the Equation (2). In the case of an open channel, the projection area is the diameter of the cylinder mulitiplied by the length of the cylinder. So the projections area will decrease as the diameter of the cylinder becomes smaller. So based on the size of the diameters of cylinders, the smallest drag force in this study is accepted by the cylinder with diameter 2 inches, both for upstream and downstream cylinders.

B. Influence of the cylinder depth level on the drag force

To test the influence of the tube depth level on the drag force, a simulation has been performed at a depth (z) that varies against a tube with a diameter of 3 inches. The drag force received at each depth can be seen in Figure 7, where the more the tube is in position, the less drag force values will be. It is consistent with the theoretical demonstrated by equation (1) and equation (2). The speed of the water particle u is influenced by the depth of the cylinder against the flat surface of water (z). The depth z is a negative value because it is below the water surface, so the more in the submerged cylinders the value z becomes smaller. In the calculation of this will reduce the value of the speed of water particles and further also will decrease the drag force value.

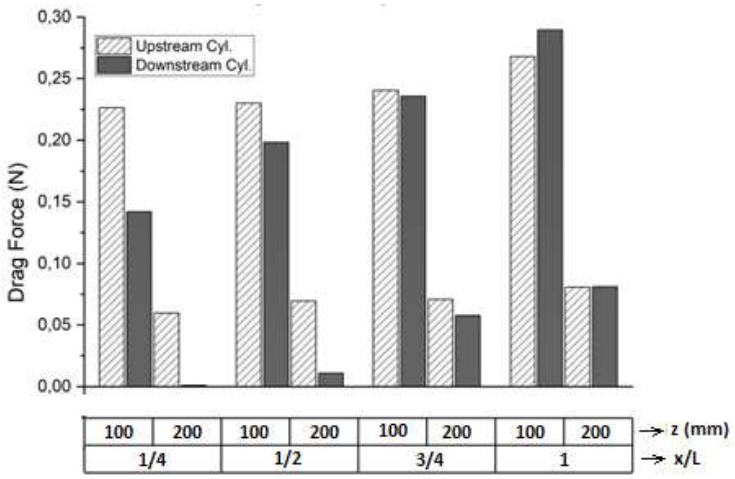

Figure 1. Graphic Value of Drag Force on Upstream and Downstream cylinders with variations in cylinder distance for Diameters 3 in at depths of: 100 mm and 200 mm.

C. Effect of cylinder spacing on streamline flow speed

The flow around the tube is significantly influenced by both the Reynolds number and the distance between the tubes (Ljungkrona and Sundén, 1993). In some studies, the ratio between the distance of the tube and the diameter of the cylinder (Igarashi, 1981; Sumner, 2010; Zdravkovich, 1977) is used. In this study, this ratio represents a comparison of x/D values. Based on Table 3, it can be seen that the Reynolds number value in this study is in the range between 1435.53 to 6270.33. The range is between point C and point D in Figure 3 and the flow characteristics are as seen in Figure 8 (Munson, 2022).

Figure 2. Flow characteristics for the Reynolds number range in this study (Munson, 2022).

If a sample of data is taken for a 3 inch cylinder diameter at a depth of 0.1m, the following Figure 9 is an image of the flow formed in this study for different centre distances between cylinders.

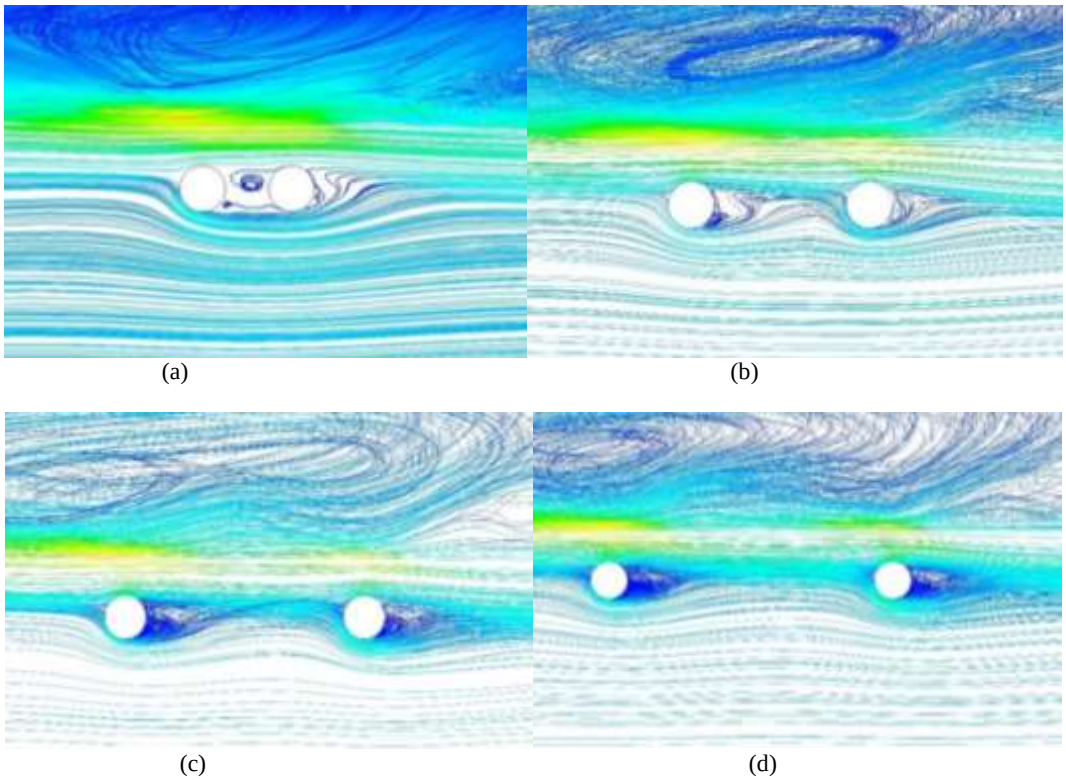

Figure 9. The streamline flow rate received by the two cylinders with the variation of the distance between the axes of the cylinder: (a) x/L = 1⁄4, (b) x/L = 1⁄2, (c) x/L = 3⁄4, and (d) x/L = 1

In Figure 9(a) with a ratio of x/D = 1.9259, the flow separated by the upstream cylinder does not accumulate back into the downstream, but directly towards the rear of the downstream cylinder due to the very close cylinder distance. The downstream cylinder undergoes a smaller pressure on the front side than on the back side because there is no flow coming from the front. For Figure 9(b) with a ratio of x/D = 3.8517, there is still a pattern similar to the Figure 9(a) but there is little flow separated (due to the upstream cylinder), which reassembles and adheres to the downstream. Under these conditions, the pressure on the front side of the cylinder downstream is greater than on the back. This indicates that the downstream cylinders are already outside the upstream cycle formation area (Ljungkrona and Sundén, 1993).

V. CONCLUSION

The force exerted on both the upstream tube and downstream tubes is influenced by the distance between them. The smaller the distance between the two cylinders, the lower the drag force experienced. The small drag force on the downstream tube is caused by the flow separation caused by the upstream tube, so that the flow becomes relatively more turbulent. Apart from that, the depth level and diameter of the tube also affect the drag force. The deeper the position of the tube, the smaller the drag force and the larger the diameter of the tube, the greater the drag force received by the tube. According to the research, when designing a Twin SFT, it's advisable to take into account the optimal spacing between the two tubes. Specifically, the recommended distance ratio x/L is 1/4 or 1/2. However, to obtain a more comprehensive Twin

SFT technology, further research is needed to expande the study, for example, studies on the influence of load and current types, dynamic analysis, mooring cable design, and others.

ACKNOWLEDGEMENT(S)

The authors would like to acknowledge Lampung University, for funding this research under the scheme of Basic Research, SPK No. 669/UN26.21/PN/2023, Date 10 April 2023.

AUTHOR CONTRIBUTIONS

F. Forghanjaya: Conceptualization, Methodology, Software, Validation, writing – original draft, Writing – review, and editing. **J. Akmal:** Supervision, writing – original draft, Writing – review, and editing. **A. Lubis:** Writing – review and editing. **H**. **Harmen:** Writing – review and editing. **M. Irsyad:** Writing – review and editing. **M. B. Ramadhan**: Software, Validation, writing – original draft, Writing – review, and editing.

REFERENCES

Adanta, D. Fattah, I. M. R. and Muhammad, N. M. (2020). Comparison of Standard k-epsilon and SST k-omega Turbulance Model for Breastshot Waterwheel Simulation. Journal of Mechanical Science and Engineering, Vol 7(2), pp. 39-44.

Akmal J., Lubis, A., Su'udi, A., Tanti, N., Nugraha, N., Fahrain, Z.A. and Hakim, P.F. (2022). Hydrodynamic forces on submerged floating tube: The effect of curvature radius and depth level. Kapal J. Ilmu Pengetah. dan Teknol. Kelaut., vol. 19, no. 1, pp. 1–8, 2022. doi: 10.14710/kapal. v19i1.44019.

ANSYS Inc., (2015). ANSYS Fluent Meshing User's Guide. vol. 15317, pp. 724–746,

ANSYS Inc., (2021). Ansys Fluent Theory Guide," vol. Release 20.

ANSYS Inc., (2022). ANSYS FLUENT User's Guide. vol. 15317, pp. 724–746,

Arthi, T. and Murugeshwari, G. (2012). Submerged Floating Tunnels. [Online]. Available: www.ijert.org

Bearman, P. W. (2011). Circular cylinder wakes and vortex-induced vibrations. J. Fluids Struct., vol. 27, no. 5–6, pp. 648–658. doi: 10.1016/j.jfluidstructs.2011.03.021.

Boccotti, P. Arena, F., Fiamma, V. and Romolo, A. (2013). Two small-scale field experiments on the effectiveness of Morison's equation. Ocean Eng., vol. 57, pp. 141–149.

Budiman, E. (2017). Construction Challenge of Submerged Floating Tunnel in Indonesia. Jurnal Teknologi Sipil, Vol 1(2), pp. 1-7.

Cheng, X., Wang, Y. and Wang, G. (2012). Hydrodynamic Forces on a Large Pipeline and a Small Pipeline in Piggyback Configuration under Wave Action. J. Waterw. Port Coast. Ocean Eng., vol. 138, pp. 394–405.

Deng, S. Ren, H., Xu, Y., Fu, S. Moan, T. and Gao, Z. (2020). Experimental study of vortex-induced vibration of a twin-tube submerged floating tunnel segment model. J. Fluids Struct., vol. 94. doi: 10.1016/j.jfluidstructs.2020.102908.

Igarashi, T. (1981). Characteristics of the Flow around two circular cylinders arranged in tandem. Bulletin of the JSME vol. 24(188), pp. 323-331.

Jiang, B. Liang, B. and Wu, S. (2018). Feasibility study on the submerged floating tunnel in Qiongzhou Strait, China. Polish Marit. Res., vol. 25, pp. 4–11. doi: 10.2478/pomr-2018-0066.

Ljungkrona L. and Sundén, B. (1993). Flow visualization and surface pressure measurement on two tubes in an inline arrangement. Exp. Therm. Fluid Sci., vol 6(1), pp. 15–27.

Mascella, M. (2020). Global Analysis of Submerged Floating Tunnels Under Hydrodynamic Loading. Thesis, Norwegian University of Science and Technology.

Morison, J. R., Johnson, J. W. and Schaaf, S. A. (1950). The Force Exerted by Surface Waves on Piles," J. Pet. Technol., vol. 2, no. 05, pp. 149–154.

Mulvany, B. A. Nicholas J., Chen, Li., Jiyuan Y. Tu. (2004). Steady State Evaluation of Two Equation RANS Turbulence Models for High Reynolds Number Hydrodynamic Flow Simulations. Final Report, Def. Sci. Technol. Organ. Dep. Defence, Aust. Government.

Munson, B. R. Young, D. F. and Okiishi, T. H. (2002). Fundamentals of fluid mechanics, John Wiley and Sons.

Popov, D., Pervaiz, F., Alqadi, M., Raza, N. and Soo Lim, S. (2018). Feasibility Study of a Submerged Floating Crossing. Multidisciplinary Project, Delft University of Technology,

Reeve, D. Chadwick, A. and Fleming, C. (2018). Coastal Engineering Processes, Theory & Design Practice, 3rd edition.

Sarpkaya, T. (2010). Wave Forces On Offshore Structure. Cambridge University Press.

Schlichting, H. (1979). Boundary -layer Theory, 7th edition. McGraw-Hill Publishing Company.

Shankar, N. J., Cheong, H.-F., and Subbiah, K. (1988). Wave Force Coefficients for Submarine Pipelines. J. Water. Port Coast. Ocean Eng., vol. 114, pp. 472–486.

Sumer, J. B. M. and FredsØe (2016). Hydrodynamics around cylindrical structures. Word Scientific, Revised Edition.

Sumner, D. (2010). Two circular cylinders in cross-flow: A review. J. Fluids Struct., vol 26(6), pp. 849–899.

Triatmodjo, B. (1999). *Buku Teknik Pantai*. Beta Offset, Yogyakarta, pp. 1–405.

Zambon, S. (2019). "Dynamic Interaction Between a Submerged Floating Tunnel and a High Speed Train: an Uncoupled Approach. Thesis, Politecnico Milano.

Zdravkovich, M. M. (1977). Review of Flow Interference Between Two Circular Cylinders in Various Arrangements. *J. Fluids Eng*. Vol 99(4): 618-633.